STEM CELLS AND DEVELOPMENT
Volume 21, Number 5, 2012

DOI: 10.1089/scd.2011.0126

Mesenchymal Stem Cells Overexpressing CXCR4 Attenuate Remodeling of Postmyocardial Infarction by Releasing Matrix Metalloproteinase-9

Wei Huang,[1,*] Tao Wang,[1,*] Dongsheng Zhang,[1] Tiemin Zhao,[1] Bo Dai,[1] Atif Ashraf,[1] Xiaohong Wang,[2] Meifeng Xu,[1] Ronald W. Millard,[2] Guo-Chang Fan,[2] Muhammad Ashraf,[1] Xi-Yong Yu,[3] and Yigang Wang[1]

Myocardial infarction (MI) results in loss of myofibers in the ischemic zone of the heart, followed by scar formation. These factors increase barriers to mobilization of mesenchymal stem cells (MSC), thereby impeding their effectiveness in cardiac repair. This study examined MSC overexpressing CXCR4 (MSC^{CX4}) to determine penetration into infarcted myocardium by releasing collagen degrading enzyme, matrix metalloproteinase-9 (MMP-9). In vitro, mouse MSC were utilized, including MSC using adenoviral transduction, to express CXCR4/green fluorescent protein (GFP) (MSC^{CX4}), Null/GFP (MSC^{Null}), MSC treated with siRNA targeting CXCR4 (MSC^{siR}), MSC treated with control siRNA($MSC^{Con\text{-}siR}$), MSC^{CX4} treated with siRNA targeting MMP-9 ($MSC^{CX4\text{-}siRMP9}$) and MMP-14 ($MSC^{CX4\text{-}siRMP14}$), MSC derived from MMP-9 knockout mouse with adenoviral transduction for GFP (MSC^{MP9-}), or MSC^{MP9-} plus overexpressing CXCR4 ($MSC^{MP9\text{-}CX4}$). The ability to cross the basement membrane was evaluated in all MSC using a trans-collagen gel invasion assay. The CXCR4 and MMP expression were analyzed by Western blot. In vivo, MSC with various treatments were infused into mice via tail vein injections 7 days after MI. Echocardiography was performed before harvesting hearts for analysis at 4 weeks after MSC injection. Both in vitro and in vivo studies demonstrated upregulation of MMP-9 induced by MSC^{CX4}, promoting increased GFP^+ cell migration into the infarcted area in comparison to control group. This enhanced response was associated with reduced left ventricular (LV) fibrosis, increased LV free wall thickness, angiogenesis, and improved LV function. Under hypoxic conditions, MMP-9 is upregulated in MSC^{CX4}, thus facilitating cross of the basement membrane, resulting in an improved remodeling of post-MI tissue.

Introduction

Progenitor/stem cell research has become a primary focus in the study of tissue regeneration given the potential benefits of using pluripotent stem cells in transplantation procedures. Singla et al. reported decreased apoptosis, hypertrophy, and fibrosis [1–3] after stem cell transplantation in the infarcted heart.

Myocardial fibrosis is a response to tissue injury wherein connective tissue deposits in the interstitial space of myocardium [4]. The accumulation of extracellular matrix (ECM) materials and fibroblasts in areas of tissue injury often impairs penetration of reparative mesenchymal stem cell (MSC)'s mobilization from peripheral reservoirs. Proteolytic enzymes such as membrane type-1 matrix metalloproteinase (MT1-MMP, namely MMP-14), MMP-2, MMP-9, and other cytokines such as hepatocyte growth factor, stromal cell-derived factor-1α (SDF-1α), and stem cell factor released by cells within injured tissues can increase the numbers of migrating progenitor cells in the circulation and attract them to damaged tissue sites [5]. Upregulation of MMP-2, MMP-9, and MMP-14 by human MSC increases vessel network formation [6].

The MMPs play a critical role in tissue remodeling by degrading the ECM and releasing growth factors and defense proteins [6]. The ECM modulates blood vessel formation by changing composition and structure to induce endothelial cell migration and formation of new capillary networks [7]. The MMPs have also demonstrated an ability to affect the progression of myocardial infarction (MI), left ventricular (LV) dilation, and heart failure after adverse coronary pathology or ischemic events [8]. In addition, MSC migration has been demonstrated to follow SDF-1α gradients [5]. The migration to injured tissue sites can be blocked by an MMP inhibitor derived from green tea (Camellia sinensis); polyphenol

Departments of [1]Pathology and Laboratory Medicine and [2]Pharmacology and Cell Biophysics, University of Cincinnati Medical Center, Cincinnati, Ohio.
[3]Medical Research Center of Guangdong General Hospital, Guangdong Academy of Medical Sciences, Guangzhou, China.
*These two authors contributed equally to this work.

epigallocatechin-3-gallate (EGCG) [9]. This evidence further implicates the role of MMPs in MSC migration, although the involvement of other specific MMPs cannot be ruled out [9]. The MMP-9 is associated with increased CXCR4 expression in $CD34^+$ cells, and MMP-14 homing of these cells to the liver is reduced by MMP inhibitors [10]. We have created MSC^{CX4} by adenovirus-mediated gene transfer [11] to take advantage of their tendency to migrate toward infarcted myocardium in response to SDF-1α up-regulation in injured areas.

In the present study, we examined the hypothesis that MSC^{CX4} recruited to ischemic myocardium attenuate the remodeling process in the postinfarction period by releasing anti-fibrotic enzyme, MMP-9. Our strategy is to use MMP-9 released by/from MSC^{CX4}, to loosen the compact collagenous tissue in advance of MSC penetration and subsequent differentiation into a capillary network.

Materials and Methods

MSC isolation, culture, and labeling

Passage 2–4 confluent MSC were obtained from male C57BL/6J mice in seed cultures and removed from the flask using 0.25% trypsin (Sigma). The AdEasy TM Vector System (Qbiogene, Inc.) was used for regenerating recombinant adenovirus according to manufacturer's instructions and prepared as previously described [12]. In brief, the primers for qPCR containing *Bg*/II (5′) and *Hind* III (3′) linkers were synthesized as follows: CXCR4 forward primer: 5′-CAGA AGA TCT GTT GCC ATG GAA CCG ATC-3′, reverse primer: 5′-CAGA AAG CTT GGG TTA GCT GGA GTG-3′; siRNA-CXCR4 forward primer: 5′-CAC CGG ATC AGC ATC GAT TCC TTC ACG AAT GAA GGA ATC GAT GCT GAT CC-3′, reverse primer: 5′-AAA AGG ATC AGC ATC GAT TCC TTC ATT CGT GAA GGA ATC GAT GCT GAT CC-3′. For transfections, MSC were seeded on 6-well plates at 5×10^3 cells/mL 24 h before treatment, thereby resulting in $\sim$60% confluence at the time of transfection. The MSC were transduced overnight by using dilutions of concentrated virus equivalent to 1×10^7 infectious units in non-fetal bovine serum (FBS) medium, and MSC were assigned to the experimental groups. Flow cytometry was used to evaluate transfection efficiency of MSC with the viral system, as recombinant adenovirus expresses both green fluorescent protein (GFP) and CXCR4 [11].

Experimental design and MSC preconditioning (in vitro)

Mouse MSC were genetically engineered using adenoviral transduction for overexpression of CXCR4/GFP (MSC^{CX4}) or Null/GFP (MSC^{Null}) alone. The MSC (2×10^6) in primary culture were randomly assigned to one of 8 experimental groups, as follows: (i) MSC^{Null}, or (ii) MSC^{CX4}, or (iii) MSC treated with siRNA targeting CXCR4 (MSC$^{siR\text{-}CX4}$), which knock down CXCR4 gene, or (iv) MSC treated with control siRNA (MSC$^{Con\text{-}siR}$), or (v) MSC^{CX4} treated with siRNA targeting MMP-9 (MSC$^{CX4\text{-}siRMP9}$), which knock down MMP-9 gene, or (vi) MSC^{CX4} treated with siRNA targeting MMP-14 (MSC$^{CX4\text{-}siRMP14}$), which knock down MMP-14 gene, or (vii) MSC derived from MMP-9 knockout mouse (MSC^{MP9-}) with adenoviral transduction for GFP, or (viii) MSC^{MP9-} with adenoviral transduction for overexpression of CXCR4/GFP (MSC$^{MP9\text{-}CX4}$). The MSC from wild-type mice served as an additional control. The MSC in each group were incubated under hypoxic conditions (5% O_2: 90% N_2: 5% CO_2) in serum-free medium for 8 h, with 30 min recovery (95% O_2: 5% CO_2). The MSC were analyzed for CXCR4 and MMP-9 expression by Western blot. These groups of MSC treated according to the in vitro protocol were then injected into the hearts via tail vein injection 7 days after left anterior descending coronary artery (LAD) ligation.

We used adenovirus-based siRNA constructs to express siRNA, to knock down CXCR4 gene and determine its role. The adenoviral system mediated transduction allowed us to introduce a stable cell line with CXCR4 knockdown by blasticidin selection. The siRNA-CXCR4 top-strand sequence: 5′-CAC CGG ATC AGC ATC GAT TCC TTC ACG AAT GAA GGA ATC GAT GCT GAT CC-3′; the bottom-strand sequence: 5′-AAA AGG ATC AGC ATC GAT TCC TTC ATT CGT GAA GGA ATC GAT GCT GAT CC-3′. To evaluate transfection efficiency, we used the BLOCK-iT™ Adenoviral RNAi Expression System with enhanced GFP (EGFP) to deliver the specific double-stranded DNA oligonucleotides (ds oligo) that encoded the target CXCR4 pre-siRNA. Briefly, 12 h before transduction, MSC were maintained in Dulbecco's modified Eagle's medium (DMEM) with 10% FBS and then supplemented with glutamine and penicillin/streptomycin in 6-well plates. Adenoviral stock (100 µL; 2×10^5 TU/mL) was added, and the cells were incubated for 8 h. The adenoviral medium was removed, and the cells were cultured in DMEM with 10% FBS until they were needed in the experimental protocol.

Knockdown of MMP-9 and MMP-14 was performed by using ON-TARGET plus SMART pool siRNA (Dharmacon) according to the manufacturer's instructions [13].

Western blotting for CXCR4 and MMP-2, -9, -14 expression

In vitro: MMP-2, -9, -14, and CXCR4 expression in MSC were analyzed using Western blot in various treatment groups after 8 h of exposure to hypoxia to determine the effects of anti-fibrotic enzymes (MMP-2, -9, and -14) on cell homing. Protein samples (30 µg) were mixed with an equal volume of sample buffer (containing 2% SDS, 100 mM Tris, 0.2% bromophenol blue, 20% glycerol, and 200 mM DTT) and boiled for 15 min before loading into each well on 10% polyacrylamide gels (Precast Gels; ISC Bioexpress). These electrophoresed proteins were transferred from the gel to the nitrocellulose membranes (Bio-Rad). Equal loading and transfer of proteins was confirmed by Ponceau's red staining. The membranes were incubated for 60 min with 5% dry milk and Tris-buffered saline to block nonspecific binding sites. Membranes were immunoblotted overnight at 4°C with antibodies against CXCR4 (1:1,000; Chemicon), MMP-2 (1:1,000; Sigma), MMP-9 (1:2,000; Chemicon), and MMP-14 (1:1,000; Chemicon) on a rocking platform overnight. After three 5 min washings, the membranes were incubated for an hour with HRP-conjugated secondary antibody, washed, and finally developed with the ECL plus kit (Bio-Rad).

Trans-collagen invasion assay

The ability of MSC to cross the basement membrane was evaluated using a surrogate basement membrane (collagen gel) followed by a Collagen Invasion Assay [9]. Briefly,

13-mm polycarbonate filters of 8-μm pore size (Costar/Nucleopore) were coated with collagen G (Biocompare) and collagen R (Gibco, Invitrogen), which were mixed at a ratio of 1:1. Mouse embryonic fibroblasts (MEF, 1×10^5) were then seeded on the gel, grown to confluence, and stained with CellTracker Red (Molecular Probes). Finally, MSC were suspended in Iscove's modified Dulbecco's medium (IMDM)/0.1% BSA at 2×10^6 cells/mL and were seeded on the top of MEF in the upper compartments (Fig. 2B). The lower compartment (blind well) of the modified Boyden chamber (Neuro Probe) was filled with IMDM supplemented with 0.1% BSA. The lower chamber solution contained SDF-1α at 100 ng/mL. The collagen gel was located between the upper and lower compartments. The MSC were incubated for 40 h at 37°C in 5% CO_2 before fixation with 4% paraformaldehyde and sliced in 8 μm. Specimens were analyzed using confocal images obtained on a Leitz DMRBE fluorescence microscope equipped with a TCS 4D confocal scanning attachment (Leica). Cells invading the collagen gel were quantified by counting 30 optical fields per well. To investigate the role of MMP-9 and 14 expression in MSC^{CX4} group on cell migration, siRNA targeting MMP-9, or MMP-14, or MSC from MMP-9 knockout mouse were employed.

Experiment design and MI model (in vivo)

Female mice were assigned to one of 7 groups ($n=6$ each) to receive either vehicle or MSC (2×10^6) via tail vein injection 7 days after LAD ligation: Group 1 = underwent an operation with loose suture around LAD (Sham); Group 2 = MI with vehicle treatment (MI); Group 3 = EGFP-transduced MSC (MSC^{Null}); Group 4 = MSC overexpressing CXCR4/EGFP (MSC^{CX4}); Group 5 = EGFP-transduced MSC treated with siRNA targeting CXCR4 ($MSC^{siR\text{-}CX4}$); Group 6 = EGFP-transduced MSC derived from MMP-9 knockout mouse (MSC^{MP9-}); and Group 7 = MSC^{MP9-} with adenoviral transduction for overexpression of CXCR4/EGFP ($MSC^{MP9\text{-}CX4}$).

In additional hearts, Western blot and quantitative analyses were performed for MMP expression in sham or infarcted area at 1, 3, and 7 days, and these MMP expressions either with MI itself, or MSC^{Null} or MSC^{CX4} treatment at 10 days after MI.

The MI model was developed in C57BL/6J female mice 8–12 weeks of age (20–25 g body weight), as previously described [14]. Briefly, mice were anesthetized by intraperitoneal injection of the mixture of ketamine (100 mg/kg body weight) and xylazine (5 mg/kg body weight). The animals were mechanically ventilated using a Mouse Ventilator (Minivent, Type 845 Germany) connected to a tracheal tube. Body temperature was maintained at 37°C throughout the surgical procedure. The heart was exposed by left-side limited thoracotomy, and the LAD was ligated with a 6–0 polyester suture 1 mm from the tip of the normally positioned left auricle. Control animals underwent LAD ligation, and only saline was injected. Four weeks after MSC injection, the animals were sacrificed, and hearts were frozen or fixed with 4% formalin solution, then processed for embedding in paraffin wax.

Immunohistochemical analysis of infarcted hearts

Immunohistochemical analyses were performed on paraffin LV sections. The stained sections were digitally imaged using an Olympus BX 41 microscope. In vivo: Hearts from each group ($n=4$) were harvested for studying EGFP distribution, and the number of GFP^+ cells per mm^2 in the infarcted area were counted to analyze the role of MSC^{CX4} in cell homing. Four fields of each section were examined for quantification. The GFP^+ cells were counted in each image by an independent observer who was blinded to experimental information. Sections were incubated with primary antibodies specific to GFP (Abcam), α-sarcomeric actin (Sigma), CD31 (Santa Cruz), and smooth muscle α-actin (SMA; Sigma), and they were treated with respective secondary antibodies [12]. Nuclei were stained with 4′,6-diamino-2-phenylindole. Blood vessel density in peri-infarcted myocardium was calculated in at least 8 randomly high power fields in each heart section. Fluorescent images were obtained with an Olympus BX 41 microscope equipped with a digital camera (Olympus).

Measurement of infarct size and LV anterior wall thickness

Fixed hearts were embedded in paraffin, and sections from mid-LV were stained with Masson's Trichrome. Fibrotic area and total LV area of each image were measured using the Image-Pro Plus (Media Cybernetics Inc.), and the percentage of the fibrotic area was calculated as shown: (fibrotic area/total LV area) ×100. The LV area images were taken of each slide by using an Olympus BX41 with CCD (MagnaFire™; Olympus) camera. The LV anterior wall thicknesses were measured by a scale bar under microscopy.

Assessment of cardiac function

The LV function variables were assessed by transthoracic echocardiography, which was performed 4 weeks after MSC transplantation using an iE33 Ultrasound System (Phillips) with a 15-MHz probe. After light general anesthesia, hearts were imaged 2-dimensionally in long-axis view at the level of the greatest LV diameter. This view was used to position the M-mode cursor perpendicular to the LV anterior and posterior walls. The left ventricle internal end-diastolic dimension (LVIDd) and left ventricle internal systolic dimension (LVIDs) were measured from M-mode recordings using the leading-edge method. The LV ejection fraction (LVEF) was calculated as follows: LVEF (%) = $[(LVIDd)^{3-}$ $(LVIDs)^3]/(LVIDd)^{3\times}$ 100. Fractional shortening (FS) was calculated as: FS (%) = (LVIDd-LVIDs)/LVIDd ×100. All echocardiography measurements were averaged from at least 4 separate cardiac cycles.

Statistical analysis

Experiments were performed in quadruplicate and repeated at least thrice. Data are expressed as mean ± standard error of the mean. Statistical significance was assessed by analysis of variance followed by Bonferroni/Dunn testing, or unpaired Student's t-test. A P value ≤ 0.05 was considered statistically significant.

Results

In vitro Studies

CXCR4 and specific MMP expression either on MSC or infarcted myocardium. The expression of CXCR4, MMP-9,

and -14 was significantly upregulated in MSC^{CX4} groups under normoxia when compared with MSC^{Null} ($^{*}P \le 0.05$) and increased further after exposure to hypoxia for 8 h (Fig. 1A). In addition, there was significant upregulation of all the genes in MSC^{Null}, MSC^{CX4}, and MSC$^{siR\text{-}CX4}$ groups under hypoxia as compared with normoxia ($^{\#}P \le 0.05$) except for MMP-2 expression, which was not significantly different in MSC^{CX4} group in comparison to the MSC^{Null}, and MSC$^{siR\text{-}CX4}$ groups after exposure to either the normoxia or hypoxia. Interestingly, this CXCR4 upregulation was significantly reduced after MSC treated with siRNA targeting CXCR4 gene. Similarly, an increased amount of MMP-9 and 14 expression was also completely abolished by knockdown CXCR4 in MSC$^{siR\text{-}CX4}$ group (see Fig. 1A).

A similar pattern as in in vitro study was also observed in heart tissue. The expression of MMP-9 at day 3 and 7 and MMP-14 at day 7 was also significantly upregulated after LAD ligation only as compared with sham group ($^{*}P \le 0.05$) except for MMP-2 (Fig. 1B), which was no significantly different at day 1, 3, and 7.

The level of MMP-2 expression was not significantly different between 2 groups (MSC^{Null} and MSC^{CX4}) at day 10 after MI. However, the level of MMP-9 and MMP-14 was significantly increased in MSC^{CX4} group in comparison with MSC^{Null} group ($P \le 0.05$) (Fig. 1B).

Role of CXCR4 and specific MMP expression on MSC migration. After exposure of MSC for 40 h to SDF-1α (100 ng/mL, Fig. 2A), cell migration was significantly increased in MSC^{CX4} group ($P \le 0.05$ vs. MSC^{Null}) and this enhanced MSC^{CX4} migration was obviously inhibited in MSC$^{siR\text{-}CX4}$ group (Fig. 2B, C), thus suggesting that CXCR4 plays an important role in cell migration. Confocal images for cell penetration at various time points in MSC^{CX4} group are illustrated in Fig. 2B (data in other groups not shown).

To determine the role of specific MMP involved in MSC^{CX4} migration, siRNA targeting MMP-9, MMP-14, or MSC from MMP-9 knockout mouse were employed. The siRNA-mediated decrease in the expression of MMP-9 and MMP-14 was confirmed by performing Western blot (Fig. 2D). Cell migration in response to SDF-1α in MSC$^{CX4\text{-}siRMP9}$ group was significantly inhibited in comparison to MSC^{CX4} group, which was similar in MSC^{MP9-}, MSC$^{MP9\text{-}CX4}$, and MSC$^{siR\text{-}CX4}$ group; whereas MSC^{CX4} treated with siRNA against MMP-14 did not affect the migration (Fig. 2C). This finding supports a mechanism in which MMP-9 release from MSC^{CX4} plays an important role in cell migration and penetration of a surrogate basement membrane (collagen gel).

In Vivo Studies

Evidence of MSC migration into the infarcted area 4 weeks after cell delivery in various treatment groups. The MSC migration in various treatment groups was analyzed by counting the number of GFP^{+} cells. There was a significantly increased number of GFP^{+} cells dispersed in the infarcted area in the MSC^{CX4} treated group over all other treatment groups (Fig. 3A, B). This result indicates that therapeutic effect of CXCR4 overexpression is dependent on MMP-9 expression in MSC.

Evidence of angiogenesis at 4 weeks after MSC injection in various treatment groups. Capillary density was visualized by using PECAM-1 (CD31), an endothelial cell marker, and was significantly higher in the MSC^{CX4} group than in MI, MSC^{Null}, MSC$^{siR\text{-}CX4}$, MSC^{MP9-}, and MSC$^{MP9\text{-}CX4}$ groups (Fig. 4A, B). Similarly, vascular density was measured by labeling SMA, a marker for vascular smooth muscle cells, and was significantly greater in MSC^{CX4} group compared to all other groups (Fig. 4C, D). These results indicate that MSC^{CX4} convey an angiogenic capacity as a part of the MI repair process.

Effect of MSC^{CX4} on fibrosis and wall thickness of left ventricle

Figure 5A shows Masson–Trichome staining for LV sections in various treatment groups. At 4 weeks after MSC injection, the MSC^{CX4} group exhibited a significant reduction (12.6% ± 2.2%) in fibrosis as compared with MI (44.3% ± 3.1%), MSC^{Null} (38.7% ± 3.9%), MSC$^{siR\text{-}CX4}$ (43.2% ± 3.7%), MSC^{MP9-} (46.9% ± 6.7%), and MSC$^{MP9\text{-}CX4}$ (44.7% ± 5.1%) groups (Fig. 5A, B). The thickness of LV free wall was greater in MSC^{CX4} groups (403.7 ± 42.5 μm) (Fig. 5C), most prominently in comparison to MI (141.7 ± 12.5 μm), MSC^{Null} (271.4 ± 29.8 μm), MSC$^{siR\text{-}CX4}$ (171.3 ± 15.7 μm), MSC^{MP9-} (128.6 ± 21.4 μm), or MSC$^{MP9\text{-}CX4}$ groups (131.4 ± 18.1 μm), (Fig. 5A, C). There was, however, no significant difference in interventricular septum thickness among the study groups. These results indicate that mobilization of MSC^{CX4} into the infarcted area reduced infarcted size and prevented or reversed ventricular remodeling subsequent to coronary artery occlusion.

The effect of MSC^{CX4} transplantation on LV dimensions and global function

Measurement of LVIDs and LVIDd in mice with MSC^{CX4} was improved compared with all other groups, $^{*}P \le 0.05$, (Fig. 6A–C). No significant differences in LVIDd were noted in MI (5.2 ± 0.2 mm), MSC^{Null} (5.0 ± 0.3 mm), MSC$^{siR\text{-}CX4}$ (5.2 ± 0.5 mm), MSC^{MP9-} (5.4 ± 0.3 mm), and MSC$^{MP9\text{-}CX4}$ (5.1 ± 0.3 mm) with the exception of MSC^{CX4} (4.4 ± 0.3 mm), which was significantly better than MSC^{Null}. The LVIDs was increased in groups of MI (4.5 ± 0.1 mm), MSC^{Null} (4.1 ± 0.3 mm), MSC$^{siR\text{-}CX4}$ (4.4 ± 0.2 mm), MSC^{MP9-} (4.6 ± 0.5 mm), and MSC$^{MP9\text{-}CX4}$ (4.2 ± 0.4 mm), showing no significant differences among the groups. Similarly, LVIDs was significantly lower in the MSC^{CX4} (3.3 ± 0.2 mm) as compared with MSC^{Null}.

The LV function as assessed by EF and FS in M-model echocardiography were significantly improved in MSC^{CX4} (55.0% ± 4.4% and 24.6% ± 1.9%, respectively) as compared with these contractile performance parameters in MSC^{Null} (43.1% ± 3.2%, 18.4% ± 2.2%, respectively, $^{*}P \le 0.05$) (Fig. 6D, E). However, LVEF was significantly reduced to 35.2% ± 2.2% in MI, 38.1% ± 2.9% in MSC$^{siR\text{-}CX4}$, 34.3% ± 4.1% in MSC^{MP9-}, and 39.1% ± 3.9% in MSC$^{MP9\text{-}CX4}$ group compared with 55.0% ± 4.4% in MSC^{CX4} group. This reduced FS level was likewise observed in MI, MSC$^{siR\text{-}CX4}$, MSC^{MP9}, or MSC$^{MP9\text{-}CX4}$ groups, which were no different from MSC^{Null}.

Discussion

Myocardial fibrosis, a hallmark of many cardiovascular diseases, is the abnormal deposition of collagenous fibers in the interstitial space of the myocardium [4]. The increase in collagenous deposition in the infarcted area presents an

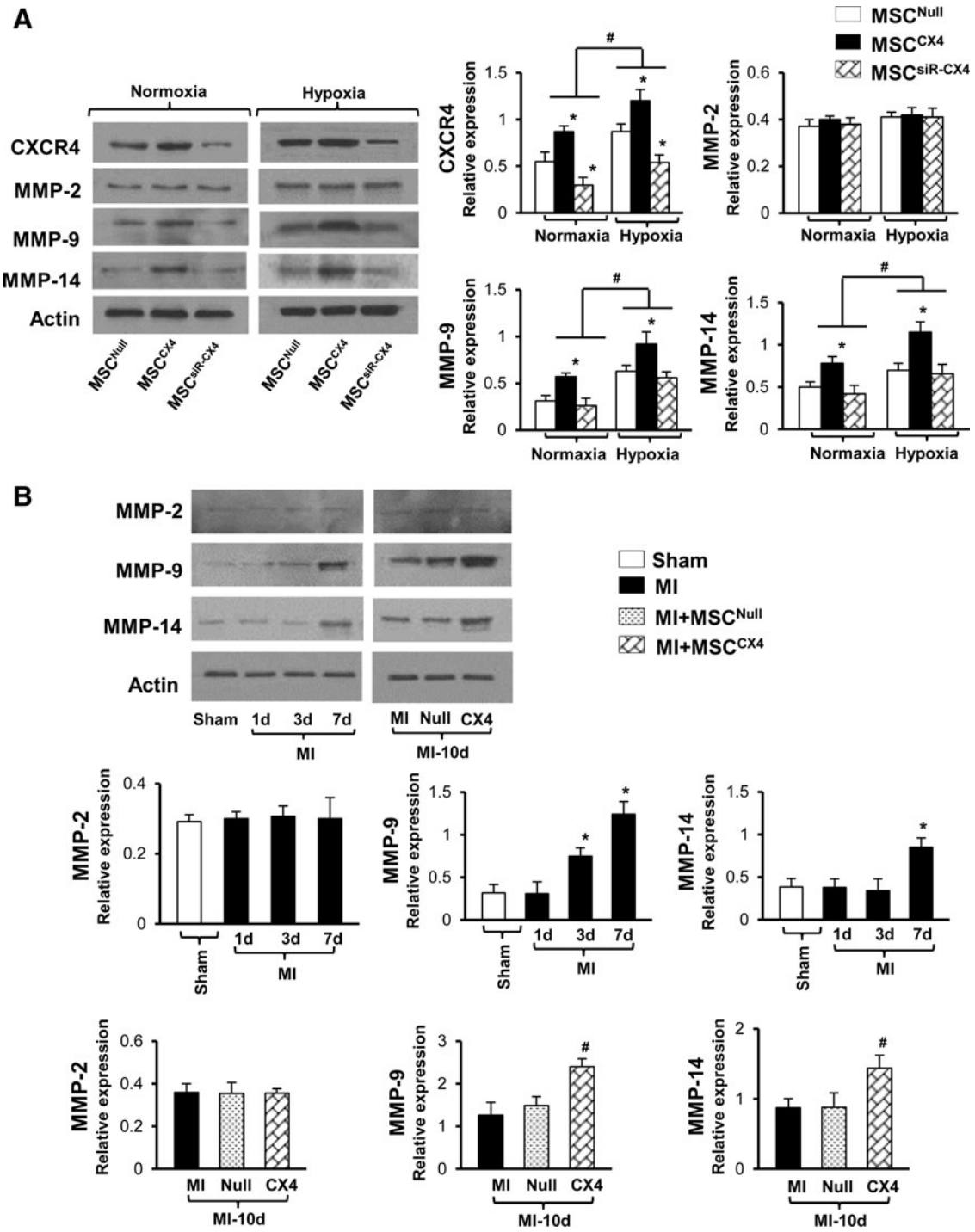

FIG. 1. CXCR4 and specific MMP expression either in MSC or infarcted myocardium. **(A)** Western blot and quantitative analyses for CXCR4, MMP-2, -9, and -14 expressions in various treatment groups under normoxic or hypoxic conditions. All values are expressed as mean ± S.E.M. $n = 6$ for each group. $^{*}P \leq 0.05$ versus MSC^{Null}, $^{\#}P \leq 0.05$ versus normoxia. **(B)** Western blot and quantitative analyses for MMP-2, MMP-9, and MMP-14 expression in sham or infarcted myocardial area at 1, 3, and 7 days, and these MMP expressions either with MI alone, or MSC^{Null} or MSC^{CX4} treatment at 10 days after MI. All values are expressed as mean ± S.E.M. $n = 6$ for each group. $^{*}P \leq 0.05$ versus Sham; $^{\#}P \leq 0.05$ versus Null. MSC^{Null}, GFP-transduced MSC; MSC^{CX4}, MSC overexpressing CXCR4/GFP; $MSC^{siR\text{-}CX4}$, GFP-transduced MSC treated with siRNA targeting CXCR4; Sham indicates operation with loose suture around LAD; MI, myocardial infarction only without cell transplantation; MI-10d, results from 10 days after MI; Null, MI with MSC^{Null} treatment; CX4, MI with MSC^{CX4} treatment; MSC, mesenchymal stem cell; MI, myocardial infarction; MMP, matrix metalloproteinase; GFP, green fluorescent protein; S.E.M., standard error of the mean; LAD, left anterior descending coronary artery.

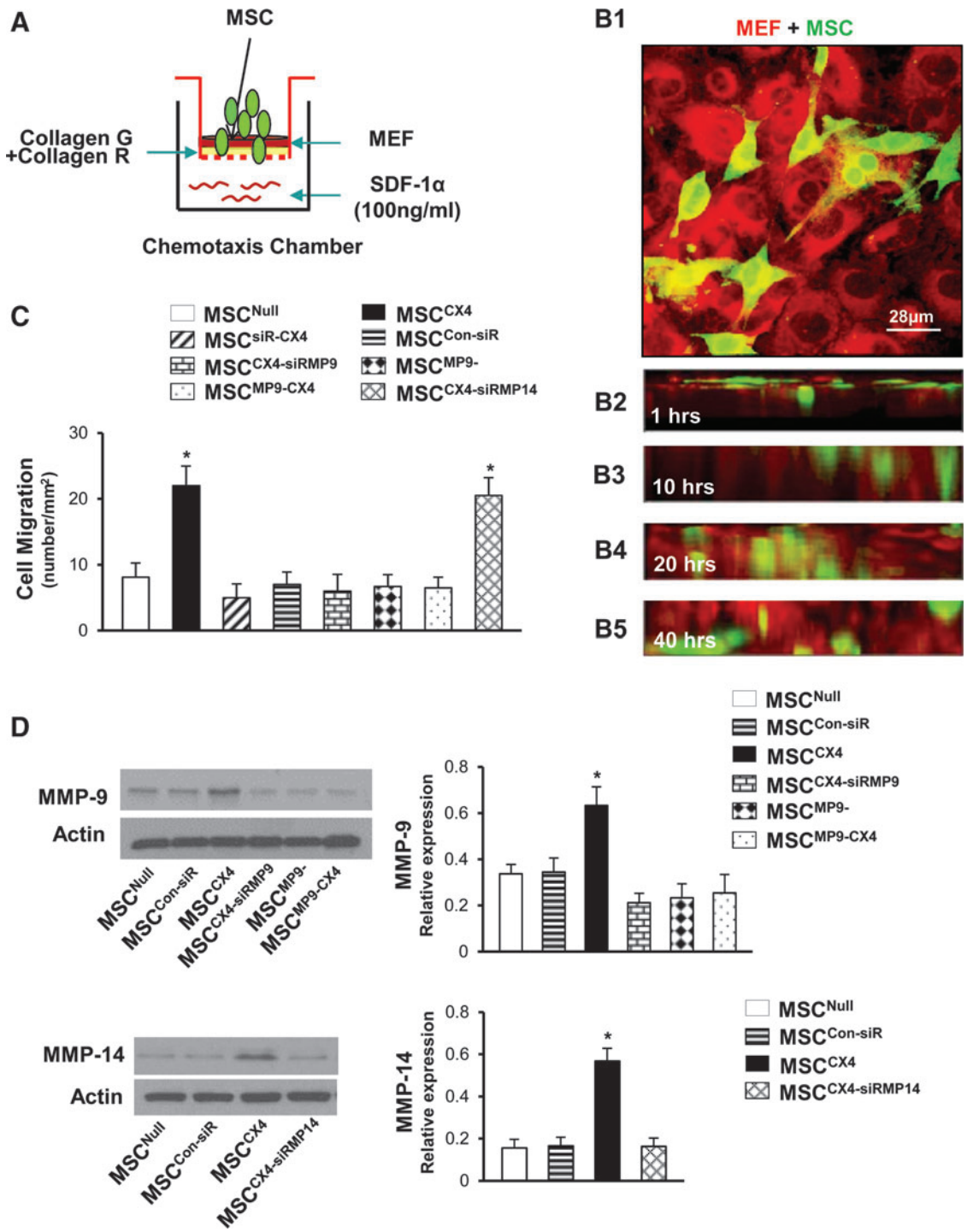

FIG. 2. Role of CXCR4 and specific MMP expression on MSC migration. **(A)** Schematic representation of chemotaxis experiments for cell migration. **(B)** Confocal images for cell penetration at various time points in MSC^{CX4} group (data in other groups not shown). MSC (green) co-cultured with monolayer MEF (red) for 20 min **(B1)**. Images in individual X-Z frames show that MSC gradually migrated from uppermost gel surface to the bottom at different time points **(B2–B5)**. Color codes given at the top. **(C)** Quantitative data for MSC migration. **(D)** Western blot and quantitative data for MMP-9 and MMP-14 in various MSC treatment groups. All values are expressed as mean ± S.E.M. $n = 6$ for each group. *$P \leq 0.05$ versus MSC^{Null}. All original magnifications is 630 × 1.4 in confocal image. MEF, mouse embryonic fibroblasts; MSC$^{Con\text{-}siR}$, MSC treated with control siRNA; MSC$^{CX4\text{-}siRMP9}$, MSC^{CX4} treated with siRNA targeting MMP-9; MSC$^{CX4\text{-}siRMP14}$, MSC^{CX4} treated with siRNA targeting MMP-14; MSC^{MP9-}, GFP-transduced MSC derived from MMP-9 knockout mouse; MSC$^{MP9\text{-}CX4}$, MSC^{MP9-} with adenoviral transduction for overexpression of CXCR4/GFP.

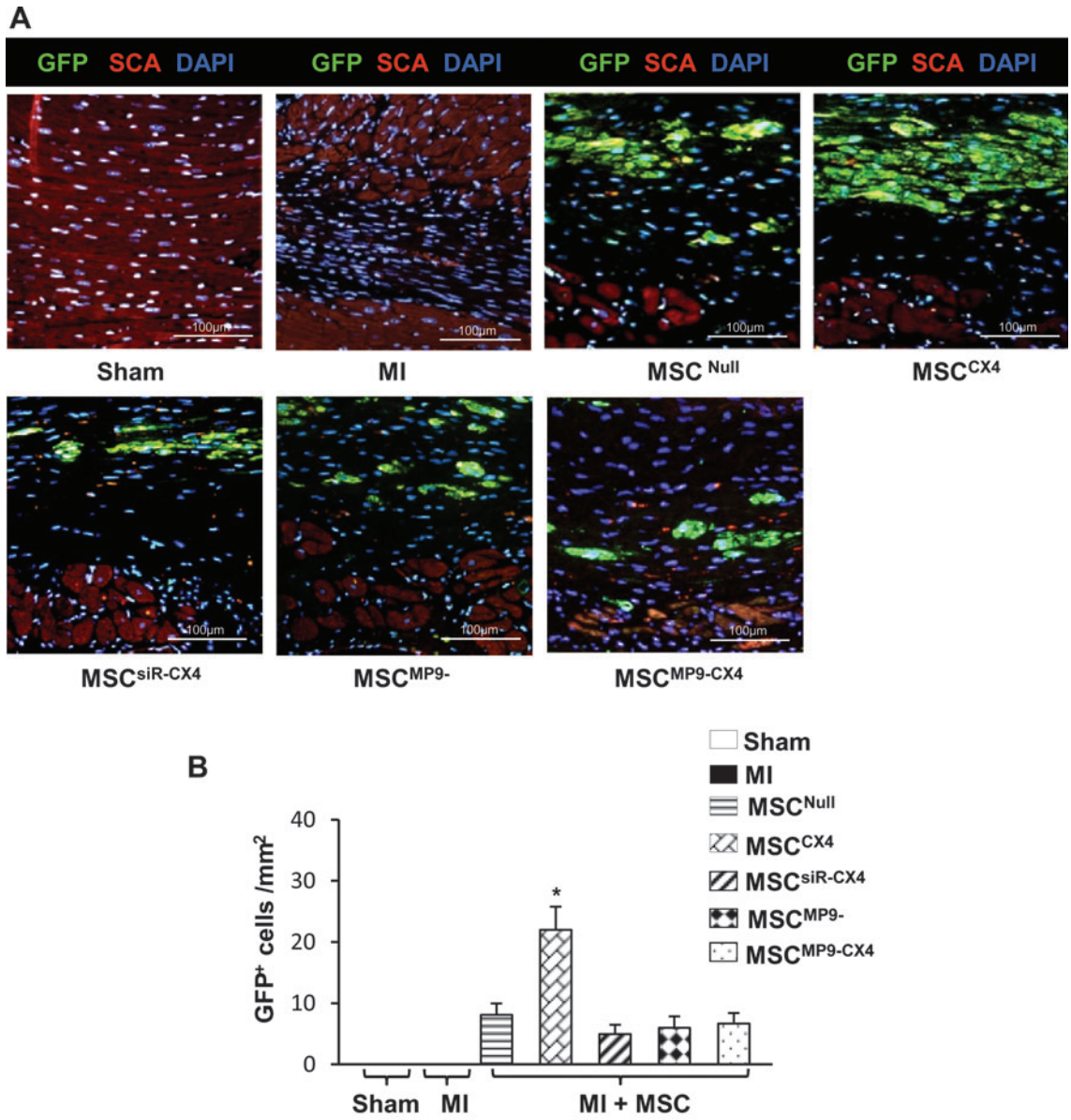

FIG. 3. MSC migration in situ at 4 weeks. **(A)** Significant number of enhanced GFP^+ cells migrated into the infarcted area in MSC^{CX4} treated group as compared with MSC^{Null} treated group. There were no significant different in the GFP^+ cell numbers in other groups except in MSC^{CX4} treated group, which showed that the number of GFP^+ cells was significantly higher than any other groups ($P \leq 0.05$ vs. MSC^{Null}). Color code given at the top. GFP, green fluorescence protein (*green color*); SCA, α-sarcomeric actin (*red color*); DAPI, (*blue color*). **(B)** Quantitative data for number of GFP^+ cells in the infracted area after 4 weeks of cell delivery. All values are expressed as mean ± S.E.M. $n = 4$ for each group.*$P \leq 0.05$ versus MSC^{Null}. All original magnifications ×400. DAPI, 4′,6-diamino-2-phenylindole.

increased barrier to engraftment and survival of mobilized MSC, as its degradation via proteolytic enzymes is a prerequisite for the invasion of MSC [9]. Small new vessel formation in a collagen-containing fibrin matrix is largely driven by MMPs; specifically by membrane-type metalloproteinase(s) [6]. We have observed that certain kinds of MMPs were upregulated in MSC^{CX4} and that hypoxia induces MMP-9 and MMP-14 expression in MSC^{CX4} [5,11]; however, the role of specific MMP involved in MSC migration is not clear.

Several major differences in this study provided a new insight complementing those findings. First, the experiment design in this study used MEF seeded Trans-Collagen Invasion Assay, which mimics fibrotic basement membrane condition in the site of MI in vitro. This allowed us to better evaluate the ability of MSC to cross the basement membrane, as it is a much stricter assay for cell migration than that previously used [11]. Second, to examine the role of specific MMP on cell migration, siRNA against MMP-9 or MMP-14 was used. In addition, we employed MSC^{MP9-} 129SvEv mice that specifically knockout the activity of MMP-9 to examine the role of MMP-9 in the migration of MSC with or without CXCR4 expression. Here, both in vitro and in vivo studies showed MMP-9 and MMP-14 upregulation in MSC^{CX4}

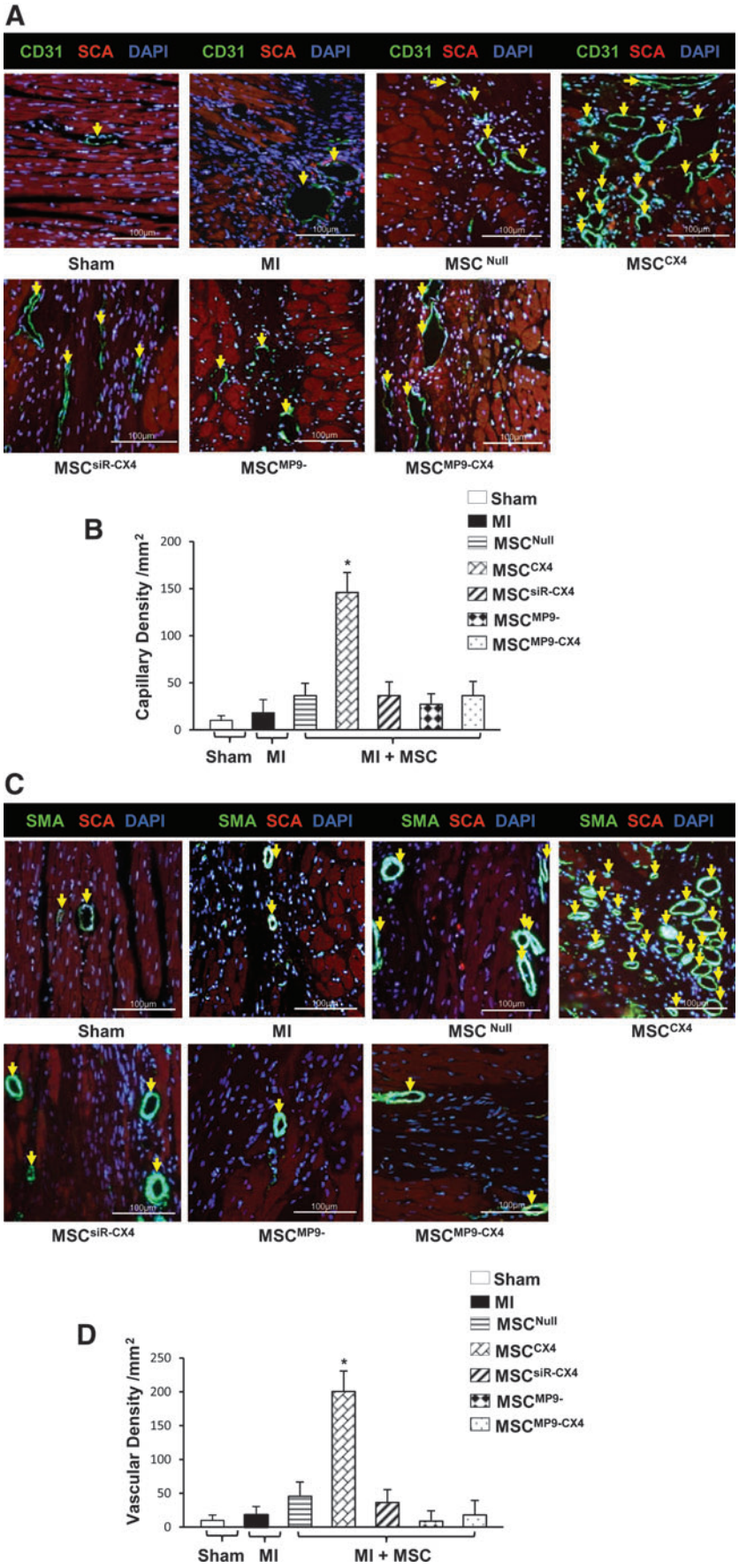

FIG. 4. Blood vessel density. Capillary density identified by CD31 antibody in various treatments **(A**, *yellow arrow*) and quantified **(B)**. Vascular density analyzed by anti-α-smooth muscle actin (SMA) antibody **(C**, *yellow arrow*) and quantified **(D)** in various treatment groups. Color code given at the top. SCA indicates α-sarcomeric actin. All values are expressed as mean ± S.E.M. $n = 6$ for each group. $^{*}P \leq 0.05$ versus MSC^{Null}. All original magnifications ×400. EGFP, enhanced green fluorescent protein.

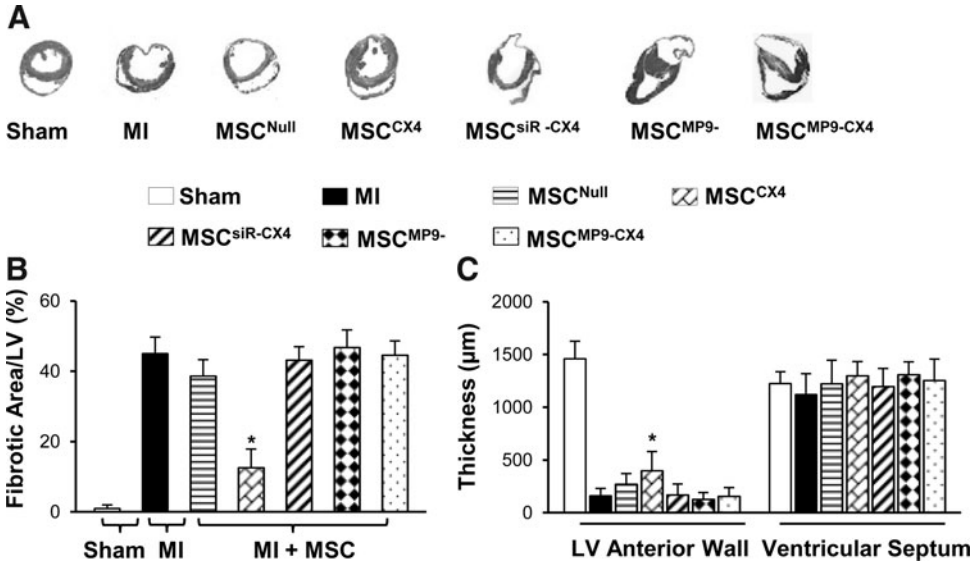

FIG. 5. Fibrosis and left ventricular (LV) anterior wall thickness. **(A)** Sections with Masson's Trichome staining. **(B)** Percentage of fibrotic area of left ventricles at 4 weeks after MSC transplantations. **(C)** LV anterior wall and septum thickness. All values are expressed as mean ± S.E.M. $n = 6$ for each group. $^*P \leq 0.05$ versus MSC^{Null}.

group; however, only knockdown of MMP-9 significantly inhibited MSC^{CX4} invasion across collagen in response to SDF-1α. This finding is consistent with Rota's study showing that cardiac restoration was governed by the ability of cardiac progenitor cells (CPCs) to synthesize MMPs that subsequently caused degradation of collagen proteins [15]. Authors of an earlier study concluded that the "CPCs form tunnels within the fibrotic tissue as they migrate across the scarred myocardium" [16]. Indeed, sufficient expression of MMP-9 was still observed in $MSC^{CX\text{-}siMP14}$, which might contribute to MSC^{CX4}-promoted invasion across collagen. In our trials, we showed that levels of MMP-2 were not significantly different between MSC^{CX4} and MSC^{Null} treatment groups, which may benefit to maintain the stability of SDF-1α, because higher levels of MMP-2 may result in decreased SDF-1α activity and block cell migration [17].

Third, our strategy in this study was to use MSC^{CX4} to increase the penetration of the compact collagenous tissue as an aid to the development of a capillary network. Angiogenesis depends on the interplay of soluble factors and cues from the ECM [18]. This process involves degradation of the basement membrane and subjacent matrix around a preexisting vessel, and endothelial cell migration and proliferation into functional tubular networks. The MMPs are a family of enzymes that contribute to ventricular remodeling and heart failure by promoting ECM degradation [19]. Unfavorable ECM remodeling leads to impaired structural support, LV dilation, increased wall stress, and heart function [20]. Our data taken together with that from other studies [21] reveal that MMP-9 expression is prominently overexpressed in the early phase after MI which correlates with fibrosis. However, the difference in our study is a focus on the role of MMP-9 in cell migration. Scar formation after MI formed a barrier against the proper integration of migrated progenitor cells and significantly hampered cell homing, engraftment, and proliferation. Thus, cells, similar to MSC^{CX4}, release anti-fibrotic enzyme (MMP-9), which is critical to penetration into an infarcted area from circulation. Besides, Jujo et al. [22] demonstrated the beneficial effect of bone-marrow-derived endothelial progenitor cells on cardiac function, which requires the MMP-9 expression in the bone marrow, but not in the ischemic region. These results are consistent with our study where heart function was not improved by transplantation of MSC derived from MMP-9 knockout mice injected into tail vein in the WT mice. This result is most likely due to the lack of MMP-9 expression in MSC derived from MMP-9 knockout mice. We observed significantly reduced cell migration in the in vitro study and decreased number of GFP positive cell migration into infarcted area. Thus, it is difficult for restoration of cardiac function after MI without MMP-9. The MMPs also degrade the ECM to facilitate tissue remodeling and release of growth factors and defense proteins [6]. The ECM modulates vessel formation by changing its composition (expressing proangiogenic integrins such as $\alpha_v ß_3$) and structure to induce endothelial cell migration and formation of new capillary networks [7]. It has been proved that MMP-9 was able to release biologically active vascular endothelial growth factor from tissue matrix [23]. Angiogenesis resulting from injury stimulus plays a key role in repairing the infarcted heart by expanding the existing vascular network. Previous study demonstrated that EGCG, a general inhibitor of MMPs, [24] inhibits angiogenesis [25]. However, the molecular mechanisms by which EGCG inhibits angiogenesis are still unclear; thus, MSC^{MP9-} 129SvEv mice employed for this study further demonstrated the important role of MMP-9 in angiogenesis.

This study has shown that the release of anti-fibrotic enzyme (MMP-9) is a critical component of MSC^{CX4} attenuated remodeling of post-MI. These enzymes might play a significant role in loosening the compact collagenous tissue permitting MSC penetration and consequent development of capillary networks. This conclusion is further supported by transplantation results, where $MSC^{MP9\text{-}CX4}$ group blunted the effect of MSC on the healing process of MI, decreased vessel formation, reduced LV remodeling and function as compared with MSC^{CX4}.

Conclusion

The present study concludes that overexpression of CXCR4 in MSC on transplantation attenuates remodeling of

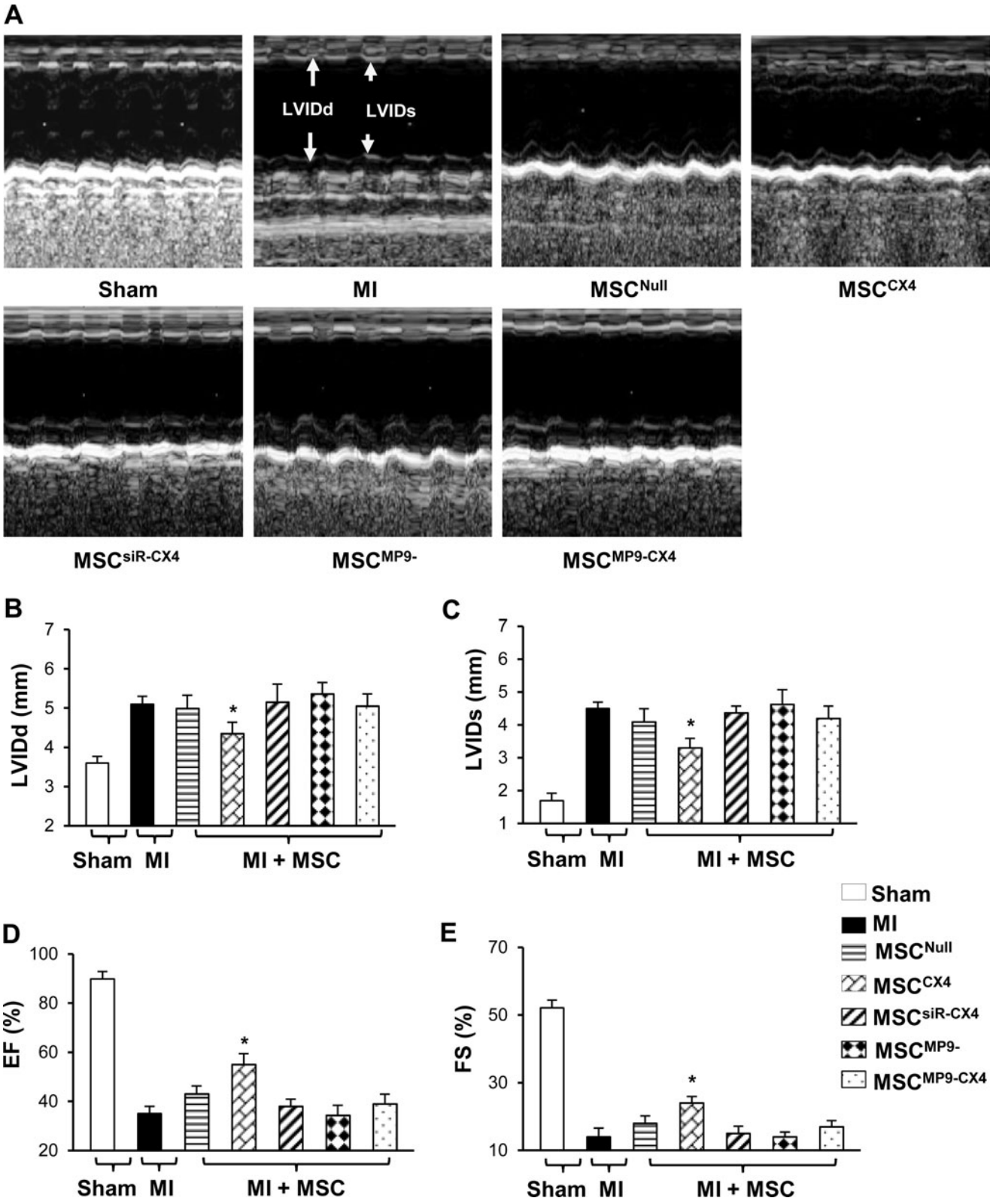

FIG. 6. Cardiac function. M-mode echocardiograms are shown at 4 weeks after MSC transplantations in various treatment groups **(A)**. Quantitative data for LVIDd **(B)**, LVIDs **(C)**, EF **(D)**, and FS **(E)**. All values are expressed as mean ± S.E.M. $n = 6$ for each group. *$P \leq 0.05$ versus MSC^{Null}. LVIDd, left ventricle internal end-diastolic dimension; LVIDs, left ventricle internal systolic dimension; EF, ejection fraction; FS, fractional shortening.

post-MI by releasing anti-fibrotic enzyme, MMP-9. This enzyme appears to loosen the compact collagenous tissue for MSC penetration by allowing proper colonization and trans-differentiation in the infarcted tissue. This strategy of exploiting MSC^{CX4} for transplantation in the infarcted myocardium would be of significant importance in future cell-based repair therapies.

Acknowledgments

This work was supported by NIH grants, HL089824 and HL081859 (Y. Wang); HL087861 (G.C. Fan); HL 087246 (M. Ashraf). The authors thank Christian Paul for the technical assistance provided.

Author Disclosure Statement

The authors indicate no potential conflicts of interest.

References

1. Singla DK, GE Lyons and TJ Kamp. (2007). Transplanted embryonic stem cells following mouse myocardial infarction inhibit apoptosis and cardiac remodeling. Am J Physiol Heart Circ Physiol 293:H1308–H1314.
2. Singla DK and DE McDonald. (2007). Factors released from embryonic stem cells inhibit apoptosis of H9c2 cells. Am J Physiol Heart Circ Physiol 293:H1590–H1595.
3. Singla DK, RD Singla and DE McDonald. (2008). Factors released from embryonic stem cells inhibit apoptosis in H9c2 cells through PI3K/Akt but not ERK pathway. Am J Physiol Heart Circ Physiol 295:H907–H913.
4. Koch A, C Geil-Bierschenk, R Rieker, TJ Dengler, FU Sack, P Schirmacher, S Hagl and PA Schnabel. (2006). Morphometric changes of the right ventricle in the first two weeks after clinical heart transplantation: analysis of myocardial biopsies from patients with complicated versus uncomplicated course. Eur J Cardiothorac Surg 30:370–378.
5. Kollet O, S Shivtiel, YQ Chen, J Suriawinata, SN Thung, MD Dabeva, J Kahn, A Spiegel, A Dar, S Samira, P Goichberg, A Kalinkovich, F Arenzana-Seisdedos, A Nagler, I Hardan, M Revel, DA Shafritz and T Lapidot. (2003). HGF, SDF-1, and MMP-9 are involved in stress-induced human $CD34^+$ stem cell recruitment to the liver. J Clin Invest 112:160–169.
6. Ghajar CM, KS Blevins, CC Hughes, SC George and AJ Putnam. (2006). Mesenchymal stem cells enhance angiogenesis in mechanically viable prevascularized tissues via early matrix metalloproteinase upregulation. Tissue Eng 12: 2875–2888.
7. Kinnaird T, E Stabile, MS Burnett, M Shou, CW Lee, S Barr, S Fuchs and SE Epstein. (2004). Local delivery of marrow-derived stromal cells augments collateral perfusion through paracrine mechanisms. Circulation 109:1543–1549.
8. Shah BH and KJ Catt. (2004). Matrix metalloproteinase-dependent EGF receptor activation in hypertension and left ventricular hypertrophy. Trends Endocrinol Metab 15:241–243.
9. Steingen C, F Brenig, L Baumgartner, J Schmidt, A Schmidt and W Bloch. (2008). Characterization of key mechanisms in transmigration and invasion of mesenchymal stem cells. J Mol Cell Cardiol 44:1072–1084.
10. Abbott JD, Y Huang, D Liu, R Hickey, DS Krause and FJ Giordano. (2004). Stromal cell-derived factor-1alpha plays a critical role in stem cell recruitment to the heart after myocardial infarction but is not sufficient to induce homing in the absence of injury. Circulation 110:3300–3305.
11. Zhang D, GC Fan, X Zhou, T Zhao, Z Pasha, M Xu, Y Zhu, M Ashraf and Y Wang. (2008). Over-expression of CXCR4 on mesenchymal stem cells augments myoangiogenesis in the infarcted myocardium. J Mol Cell Cardiol 44:281–292.
12. Pasha Z, Y Wang, R Sheikh, D Zhang, T Zhao and M Ashraf. (2008). Preconditioning enhances cell survival and differentiation of stem cells during transplantation in infarcted myocardium. Cardiovasc Res 77:134–142.
13. Renault MA, J Roncalli, J Tongers, T Thorne, E Klyachko, S Misener, OV Volpert, S Mehta, A Burg, C Luedemann, G Qin, R Kishore and DW Losordo. (2010). Sonic hedgehog induces angiogenesis via Rho kinase-dependent signaling in endothelial cells. J Mol Cell Cardiol 49: 490–498.
14. Wang Y, HK Haider, N Ahmad, M Xu, R Ge and M Ashraf. (2006). Combining pharmacological mobilization with intramyocardial delivery of bone marrow cells over-expressing VEGF is more effective for cardiac repair. J Mol Cell Cardiol 40:736–745.
15. Rota M, ME Padin-Iruegas, Y Misao, A De Angelis, S Maestroni, J Ferreira-Martins, E Fiumana, R Rastaldo, ML Arcarese, TS Mitchell, A Boni, R Bolli, K Urbanek, T Hosoda, P Anversa, A Leri and J Kajstura. (2008). Local activation or implantation of cardiac progenitor cells rescues scarred infarcted myocardium improving cardiac function. Circ Res 103:107–116.
16. Sabeh F, I Ota, K Holmbeck, H Birkedal-Hansen, P Soloway, M Balbin, C Lopez-Otin, S Shapiro, M Inada, S Krane, E Allen, D Chung and SJ Weiss. (2004). Tumor cell traffic through the extracellular matrix is controlled by the membrane-anchored collagenase MT1-MMP. J Cell Biol 167: 769–781.
17. Segers VF, T Tokunou, LJ Higgins, C MacGillivray, J Gannon and RT Lee. (2007). Local delivery of protease-resistant stromal cell derived factor-1 for stem cell recruitment after myocardial infarction. Circulation 116:1683–1692.
18. McNamee HP, HG Liley and DE Ingber. (1996). Integrin-dependent control of inositol lipid synthesis in vascular endothelial cells and smooth muscle cells. Exp Cell Res 224:116–122.
19. Spinale FG. (2002). Matrix metalloproteinases: regulation and dysregulation in the failing heart. Circ Res 90: 520–530.
20. Sutton MG and N Sharpe. (2000). Left ventricular remodeling after myocardial infarction: pathophysiology and therapy. Circulation 101:2981–2988.
21. Krishnamurthy P, J Rajasingh, E Lambers, G Qin, DW Losordo and R Kishore. (2009). IL-10 inhibits inflammation and attenuates left ventricular remodeling after myocardial infarction via activation of STAT3 and suppression of HuR. Circ Res 104:e9–e18.
22. Jujo K, H Hamada, A Iwakura, T Thorne, H Sekiguchi, T Clarke, A Ito, S Misener, T Tanaka, E Klyachko, K Kobayashi, J Tongers, J Roncalli, Y Tsurumi, N Hagiwara and DW Losordo. (2010). CXCR4 blockade augments bone marrow progenitor cell recruitment to the neovasculature and reduces mortality after myocardial infarction. Proc Natl Acad Sci USA 107:11008–11013.
23. Hawinkels LJ, K Zuidwijk, HW Verspaget, ES de Jonge-Muller, W van Duijn, V Ferreira, RD Fontijn, G David,

DW Hommes, CB Lamers and CF Sier. (2008). VEGF release by MMP-9 mediated heparan sulphate cleavage induces colorectal cancer angiogenesis. Eur J Cancer 44:1904–1913.
24. Yamakawa S, T Asai, T Uchida, M Matsukawa, T Akizawa and N Oku. (2004). (-)-Epigallocatechin gallate inhibits membrane-type 1 matrix metalloproteinase, MT1-MMP, and tumor angiogenesis. Cancer Lett 210:47–55.
25. Robinet A, A Fahem, JH Cauchard, E Huet, L Vincent, S Lorimier, F Antonicelli, C Soria, M Crepin, W Hornebeck and G Bellon. (2005). Elastin-derived peptides enhance angiogenesis by promoting endothelial cell migration and tubulogenesis through upregulation of MT1-MMP. J Cell Sci 118:343–356.

Address correspondence to:
Dr. Yigang Wang
Department of Pathology and Laboratory Medicine
University of Cincinnati Medical Center
231 Albert Sabin Way
Cincinnati, OH 45267-0529

E-mail: yi-gang.wang@ uc.edu

Received for publication March 18, 2011
Accepted after revision June 10, 2011
Prepublished on Liebert Instant Online June 14, 2011